Available online at www.sciencedirect.com

ScienceDirect

Nuclear and Particle Physics Proceedings 273–275 (2016) 1330–1333

www.elsevier.com/locate/nppp

High statistics measurement of the $K^+ \to \pi^0 e^+ \nu$(Ke3) decay formfactors

V.Obraztsov, on behalf of the "OKA" collaboration

Institute for High Energy Physics, Protvino, Moscow region Russian Federation

Abstract

The decay $K^+ \to \pi^0 e^+ \nu(K_{e3})$ is studied using in-flight decays detected with 'OKA' spectrometer. About 6M events are collected for the analysis.The λ_+ slope parameter of the decay formfactor $f_+(t)$ in the linear approximation (average slope) is measured: $\lambda_+ = (29.86 \pm 0.2) \times 10^{-3}$. If the quadratic term is added to the parametrization, the result for the linear slope becomes: $\lambda'_+ = (24.6 \pm 0.7) \times 10^{-3}$, the quadratic coefficient in this fit is $\lambda''_+ = (2.05 \pm 0.3) \times 10^{-3}$. Several alternative parametrizations are tried: the Pole fit parameter is found to be: $M_V = 891 \pm 3$ MeV ; the parameter of the Dispersive parametrization is measured to be $\Lambda_+ = (24.6 \pm 0.17) \times 10^{-3}$. All the results are very preliminary, the systematics effects are under study.

Keywords: kaon decay, formfactor, formfactor parametrization, linear slope, quadratic slope, Pole parametrization, Dispersive parametrization

1. Introduction

The decay $K \to e\nu\pi$ (K_{e3}) provides unique information about the dynamics of the strong interactions. It has been a testing ground for such theories as current algebra, PCAC, Chiral Perturbation Theory (ChPT) etc. Another possible direction is a search for new physics, namely Tensor and Scalar interactions. In this talk we present a high-statistics study(~ 6M events) of the Dalitz plot density for this decay.

2. OKA beam and detector

OKA is the abbreviation for 'Experiments with Kaons '. OKA beam is a RF-separated secondary beam of U-70 Proton Synchrotron of IHEP, Protvino. The beam is described elsewhere [1]. RF-separation with Panofsky scheme is realised. It uses two superconductive Karsruhe-CERN SC RF deflectors [2], donated by CERN. Sophisticated cryogenic system, built at IHEP [3] provides superfluid He for cavities cooling. The main beam parameters are presented in Table 1. The OKA setup is a magnetic spectrometer, presented on Fig 1. It includes:

1. Beam spectrometer on the basis of 7 1mm pitch PC's($BPC_{x,y}$) ~1500 channels in total, 4 2mm-thick scintillation counters and 2 threshold Cherenkov counters.
2. Decay volume(DV) with Veto system, 11m long, filled with He, veto system is composed of 670 Lead-Scintillator sandwiches 20× (5mm Sc +1.5mm Pb) with WLS readout. The counters are grouped in 300 ADC channels.
3. Main magnetic spectrometer: 200×140 cm^2 aperture magnet with $\int Bdl$ ~ 1 Tm; 5K 2mm pitch PC's; 1K 9mm Straw's and 300 channels of 40 mm DT's.
4. Gamma detectors: GAMS-2000(~ 2000 $4 \times 4 cm^2$ Lead glass blocks), large angle detector(EGS) (~ 1500 $5 \times 5 cm^2$ Lead glass blocks).
5. Muon detector: GDA-100 Hadron Calorimeter(100 $20x20 cm^2$ Iron-Scintillator sandwiches with WLS -plates readout); $4 \times 1 m^2$ Sc counters behind GDA-100.

http://dx.doi.org/10.1016/j.nuclphysbps.2015.09.213

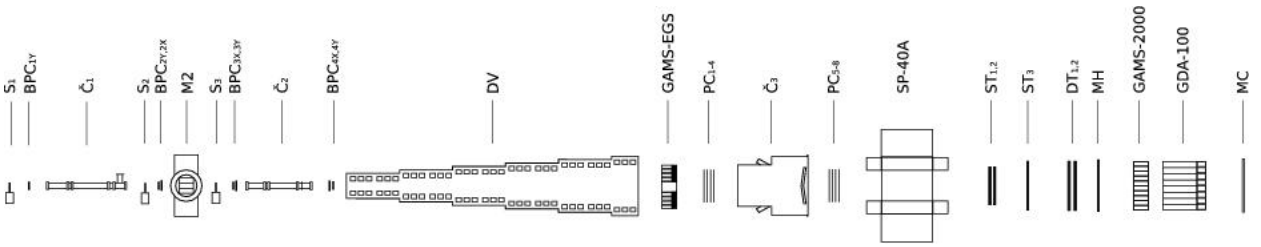

Figure 1: OKA setup

Table 1: Main parameters of the OKA beam

Primary proton beam energy	50-65 GeV/c
Primary proton beam intensity	10^{13} ppp
Secondary beam momentum	12.5 or 17.7 GeV/c
Length of the beamline	~200 m
K^+ intensity at the end	~ 10^6
% of K^+ in the beam	up to 20 %

Table 2: Statistics, taken by OKA in 2010-2013

Period	Nov10	Nov11	Nov12	Apr13	Tot
Beam p, GeV/c	12.5;17.7	17.7	12.5;17.7	17.7	
Live kaon, 10^9	6.2	5.1	17.4	12.2	40.9
$K_{\pi 2}$, 10^6	15.2	15.5	61	42	134
K_{e3}, 10^6	2.5	2.0	8.1	~ 5	~ 17

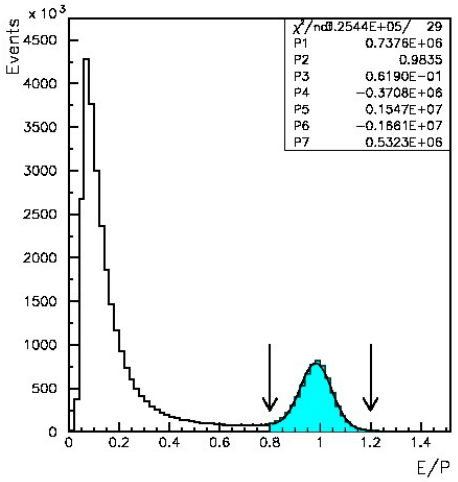

Figure 2: The ratio of the energy of the associated ECAL cluster to the momentum of the charged track(E/P plot).

3. Trigger and statistics

Very simple trigger,which is almost ″minimum bias ″ one, has been used during data-taking:

$Tr = S_1 \cdot S_2 \cdot S_3 \cdot \overline{\check{C}}_1 \cdot \check{C}_2 \cdot \overline{S}_{bk} \cdot (\Sigma_{GAMS} > MIP)$. It is a combination of beam Sc counters, $\check{C}_{1,2}$ threshold Cerenkov counters($\check{C}_1$ sees pions, $\check{C}_2$- pions and kaons), S_{bk} -a ″beam-killer ″ counter located in the beam-hole of the GAMS gamma-detector. $\Sigma_{GAMS} > MIP$ is a requirement for the analog sum of amplitudes in the GAMS-2000 to be higher than a MIP signal.

The ″OKA″ is taking data since 2010, the available statistics is shown in Table 3. In the present study we present use part of the statistics taken in 2011 and 2012.

4. K_{e3} decay selection.

The data processing starts with the beam particle reconstruction in $BPC_1 \div BPC_4$, then the secondary tracks are looked for in $PC_1 \div PC_8$; $ST_1 \div ST_3$; $DT_1 \div DT_2$ and events with one good positive track are selected. The decay vertex is searched for, and a cut is introduced on the matching of incoming and decay track. The next step is to look for showers in GAMS-2000 and EGS calorimeters. The matching of the charged track and a shower in GAMS is done on the basis of the distance r between the track extrapolation to the ECAL and the shower coordinates ($r \leq 3$cm). The electron identification is done using the ratio of the energy of the shower to the momentum of the associated track. The E/p distribution is shown in Fig 2. The particles with $0.8 < E/p < 1.2$ are accepted as electrons. The events with one charged track identified as electron and two additional showers in ECAL are selected for further processing. The mass spectrum of $\gamma\gamma$ is shown in Fig 3. The π^0 peak is situated at $M_{\pi 0} = 134.9 MeV$ with a resolution of ~ 8.5 MeV. To fight the main background from $K_{\pi 2}$ decay, the angle between the momentum of the beam kaon $\vec{p_K}$ and that of the $e\pi$-system i.e. $\vec{p_e} + \vec{p_\pi}$ is considered, see Fig 4. The background is clearly seen as a peak at zero angle.

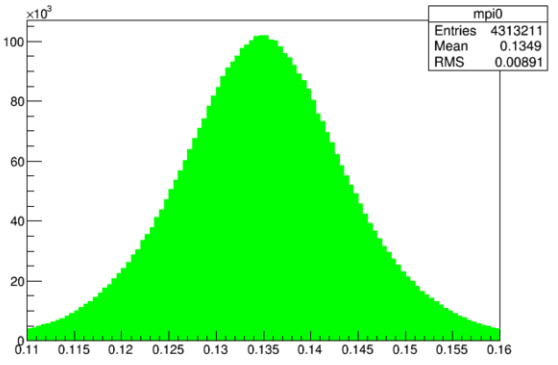

Figure 3: The $\gamma\gamma$ mass spectrum for the events with the identified electron and two extra showers.

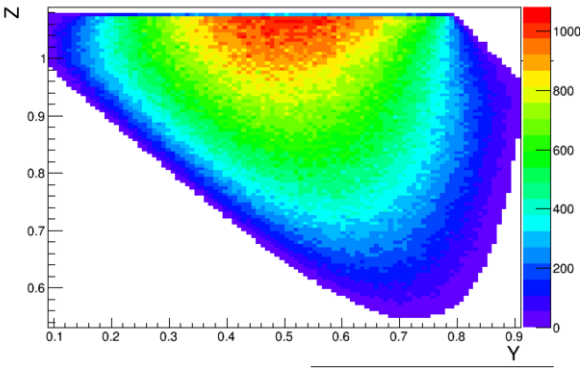

Figure 5: Dalitz plot for the selected 6M Ke3 events.

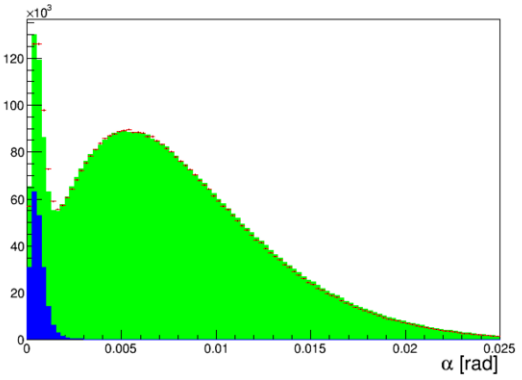

Figure 4: α- the angle between $\vec{p}_K$ and $\vec{p}_e + \vec{p}_\pi$ in the lab-system.

The cut is $\alpha > 2$mrad. Further selection is done by the requirement that the event passes 2C $K \to e\nu\pi^0$ fit. The surviving background is estimated from MC to be less than 1%.

5. Analysis

The event selection described in the previous section results in ~6M events. The distribution of the events over the Dalitz plot is shown in Fig 5. The variables $y = 2E_e^*/M_K$ and $z = 2E_\pi^*/M_K$, where E_e^*, E_π^* are the energies of the electron and π^0 in the kaon c.m.s are used. The background events, as MC shows, occupy the peripheral part of the plot. The most general Lorentz invariant form of the matrix element for the decay $K^+ \to l^+\nu\pi^0$ is [4]: $M = \frac{-G_F V_{us}}{2}\bar{u}(p_\nu)(1+\gamma^5)[((P_K+P_\pi)_\alpha f_+ + (P_K-P_\pi)_\alpha f_-)\gamma^\alpha - 2m_K f_S - i\frac{2f_T}{m_K}\sigma_{\alpha\beta}P_K^\alpha P_\pi^\beta]v(p_l)$
It consists of scalar, vector and tensor terms. $f_\pm$ are the functions of $t = (P_K - P_\pi)^2$. In the Standard Model (SM) the W-boson exchange leads to the pure vector term. The term in the vector part, proportional to f_- is reduced(using the Dirac equation) to a scalar form-factor, proportional to $(m_l/2m_K)f_-$ and is negligible in the case of K_{e3}. Different parametrizations have been used for $f_+(t)$. First is just a Taylor series: $f_+(t) = f_+(0)(1 + \lambda'_+ t/m_\pi^2 + \frac{1}{2}\lambda''_+ t^2/m_\pi^4)$. It is usually used to compare with ChPT predictions. Alternative parametrization is the pole one: $f_+(t) = f_+(0)\frac{m_V^2}{m_V^2 - t}$. The last is a relatively new Dispersive parametrization [5]: $f_+(t) = f_+(0)exp(\frac{t}{m_\pi^2}(\Lambda_+ + H(t)))$. Here H(t) is a known function.

The procedure for the experimental extraction of the parameters λ_+, f_S, f_T, which was developed in [6], starts from the Dalitz plot region $y = 0.12 \div 0.92; z = 0.55 \div 1.075$ subdivision into 100×100 cells. One can observe that the Dalitz-plot density function $\rho(y,z)$ obeys a property of quasi-factorization, i.e $\rho(y,z) = \sum_\alpha F_\alpha(\lambda'_+, \lambda''_+, f_s, f_T) \cdot K_\alpha(y,z)$. K_α are kinematic functions,which does not depend on $\lambda'_+, \lambda''_+, f_s, f_T$. The signal MC is generated with constant matrix element and $K_\alpha(y,z)$ used as weights(y,z are MC-truth values). For each α the sums of $K_\alpha(y,z)$ over events are accumulated in the Dalitz plot bins (i,j), to which the MC events fall after the reconstruction. As a result, every bin in the Dalitz plot gets weights $W_\alpha(i,j)$ and the density function r(i,j) which enters into the fitting procedure is constructed: $r(i,j) = \sum_\alpha F_\alpha(\lambda'_+, \lambda''_+, f_s, f_T) \cdot W_\alpha(i,j)$. This procedure allows to avoid systematic errors due to the "migration" of the events over the Dalitz plot because of the finite experimental resolution. To take into account the finite number of MC events, we minimize a $-\mathcal{L}$ function defined as [7]:

Table 3: The results of the fits of the $f_+(t)$, f_S, f_T formfactors.

$\lambda'_+ \times 10^3$	$\lambda''_+ \times 10^3$	$f_S/f_+(0) \times 10^2$	$f_T/f_+(0) \times 10^2$
29.86± 0.2	0	0	0
24.6 ± 0.7	2.05± 0.3	0	0
24.6 ± 0.7	2.05 ± 0.3	-0.3 ± 0.13	0
24.6 ± 0.7	2.05 ± 0.3	0	-1.3 ± 0.5

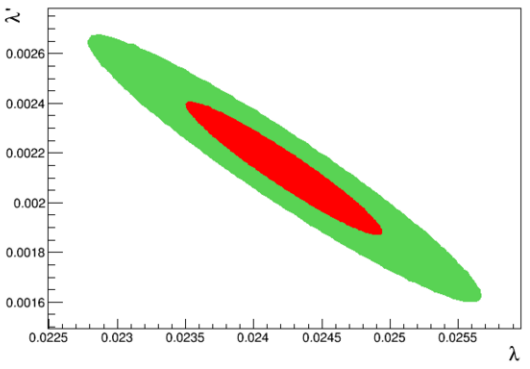

Figure 6: $\lambda' - \lambda''$ correlation plot. 1σ and 2σ contours are shown

$$\mathcal{L} = -2\sum n_j ln[\tfrac{n_j}{r_j}(1 - \tfrac{1}{m_j+1})] + (n_j + m_j + 1)ln(\tfrac{1+\frac{r_j}{m_j}}{1+\frac{n_j}{m_j+1}})$$

where the sum runs over all populated cells of the Dalitz plot, and n_j, r_j, m_j are the number of data events, the fitting function, and MC events in j-th cell.
The radiative corrections were taken into account by reweighting every MC event, according to [8].

6. Results and comparison with theory

The results of the fit are summarized in the Table 3.The first line is just a linear fit, it gives average slope of the $f_+(t)$ formfactor. The result could be compared to quite old $ChPT\ O(p^4)$ result [9]:
$\lambda_+^{ChPT} = (31.0 \pm 0.6) \times 10^{-3}$. The second line is the "standard" fit with two parameters- linear and quadratic slopes. The quadratic term is quite significant, there is a correlation between parameters as it is seen on Fig 6. The $ChPT\ O(p^6)$ prediction for the quadratic slope is [10]: $\lambda''_+(ChPT) = (1.1 \pm 0.1) \times 10^{-3}$.

The quality of the fit is illustrated by the z and y projections of the Dalitz plot, shown on Fig 7. The third and fourth lines of the Table 3 correspond to the fits, when on top of the standard V-A term the scalar or tensor terms are allowed. It is seen, that f_S and f_T are not significant, i.e can provide upper limits.

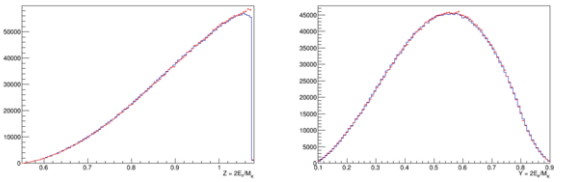

Figure 7: Projections of the Dalitz-plot on z(left) and y(right) axis. Data is the points with errors; histogram is the fit,corresponding to the 2-nd line of the Table 3.

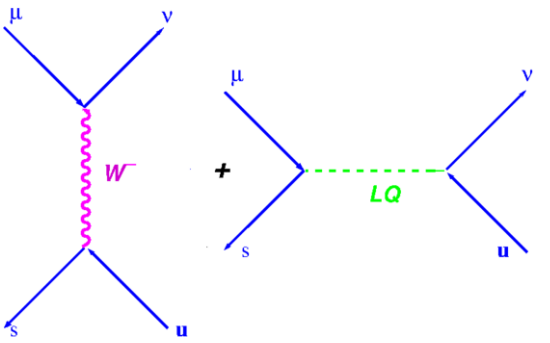

Figure 8:

The result of the Pole fit is: $M_V = 891 \pm 3$ MeV. It can be compared to the PDG value for the mass of K^* [11]: $M_{K*} = 891.66 \pm 0.26$ MeV.
The Dispersive fit gives $\Lambda_+ = (24.46 \pm 0.17) \times 10^{-3}$.
An interpretation of limits on F_S and F_T is possible in the framework of the scalar LeptoQuark(LQ) model. Then a diagram with LQ exchange should be added to the SM diagram with W (Fig 8). Applying Fiertz transformation to the LQ matrix element we get: $(\bar{s}\mu)(\bar{\nu}u) = -\frac{1}{2}(\bar{s}u)(\bar{\nu}\mu) - \frac{1}{8}(\bar{s}\sigma_{\alpha\beta}u)(\bar{\nu}\sigma^{\alpha\beta}\mu)$. The first term is the scalar, the second one - tensor. The relation between f_S, f_T and the Leptoquark scale Λ_{LQ} can be set out ([12]), as a result, a 95% lower limit for the LeptoQuark scale is $\Lambda_{LQ} > 3.5$ TeV.

References

[1] V.I.Garkusha et al., IHEP preprint IHEP 2003-4.
[2] A.Citron et al., Nucl. Instr. and Meth. 164 (1979) 31.
[3] A. Ageev et al., Proceedings of RUPAC-2008, p.282.
[4] H.Steiner et al., Phys.Lett.B36(1971)521.
[5] V.Bernard et al., Physics Letters B638(2006)480; V.Bernard et al.,Phys.Rev.D80(2009)034034.
[6] O.P.Yushchenko et al.,Phys.Lett.B589(2004)111.
[7] L.Rosselet et al., Phys.Rev.D15(1977)574.
[8] V.Cirigliano et al., Eur.Phys.J.C23(2002)121.
[9] J.Gasser and H.Leutwyler, Nucl. Phys. B250(1985)517.
[10] J.Bijnens,P.Talavera, Nucl. Phys. B669(2003)341.
[11] K.A.Olive et al.,Chin.Phys.C,**38**,090001(2014).
[12] V.V.Kiselev et al., hep-ph/0204066/